RSC Advances

ROYAL SOCIETY OF CHEMISTRY

www.rsc.org/advances

Journal Name

RSCPublishing

ARTICLE

Tough and VEGF-releasing scaffolds composed of artificial silk fibroin mats and natural acellular matrix

Cite this: DOI: 10.1039/x0xx00000x

Received 00th January 2012,
Accepted 00th January 2012

DOI: 10.1039/x0xx00000x

www.rsc.org/

Zhaobo Li, [a] Lujie Song, [b] Xiangyu Huang, [a] Hongsheng Wang, [c] Huili Shao, [a] Minkai Xie, [b] Yuemin Xu, *[b] and Yaopeng Zhang *[a]

Regenerated silk fibroin (RSF) scaffolds electrospun from aqueous solutions have great potentials for tissue engineering. However, the traditional RSF mats are weak and limit the applications. Bladder acellular matrix graft (BAMG), a tough natural material, was used as an electrospinning substrate to toughen the RSF scaffolds. Compared with bare RSF scaffolds, the composite scaffolds with breaking energies ranging from 458 to 970 $J \cdot kg^{-1}$ show significantly improved tensile properties and suture retention strength, which may satisfy the requirements for implantation. Vascular endothelial growth factor (VEGF) was encapsulated in the RSF/BAMG composite scaffolds by means of blend and coaxially electrospinning to promote the ability of vasculogenesis and angiogenesis. Transmission electron microscope (TEM) images show that the coaxially electrospun fibers had a core-sheath structure. ELISA assay measurement indicates that VEGF can release more than 16 days. The samples annealed in water vapor exhibit higher release profiles than those immersed in ethanol. *In vitro* assay indicates that VEGF loaded scaffolds evidently induced the attachment and proliferation of porcine iliac endothelial cells (PIECs) compared with those without VEGF. Moreover, the VEGF remained bioactive for up to 7 days. Thus the VEGF loaded composite scaffolds could be a promising candidate for tissue engineering applications.

1.Introduction

Tissue engineering (TE) aims at developing functional substitutes for damaged or diseased tissues and organs. Suitable TE scaffolds serve as a mimic for the native extracellular matrix (ECM) whose structures are based on biocompatible and biodegradable materials. Natural ECM can not only support cell attachment, morphogenesis, migration, proliferation and differentiation, but also deliver biochemical factors.[1-3] Among the methods to fabricate TE scaffolds, electrospinning has emerged to be a simple and effective technique to fabricate nano- or micrometric fibers with a consequent large surface-to-volume ratio which has a similar structure of the electrospun fibers to the natural ECM. [4-8]

Silkworm silk from *Bombyx mori* has been used as suture for centuries.[9] During decades of investigation, silk has effectively proven to be a useful biomaterial in many clinical applications due to its good properties, such as environmental stability, biocompatibility, anti-bacterial property, tailorable biodegradability, good oxygen/water vapor permeability and low inflammatory response.[10-13] Therefore, electrospun regenerated silk fibroin (RSF) fibers have been investigated widely for their potential applications as TE scaffolds.[14-16] However, most electrospun RSF scaffolds are prepared from organic solvents such as formic acid,[17-19] hexafluoroisopropanol (HFIP)[20-22] and hexafluoroacetone (HFA),[23] which are toxic and unfriendly to humans and environment. The residual solvents in the scaffolds are also very likely harmful. Therefore, our group and other researchers have used water as solvent to prepare electrospun RSF scaffolds instead of the organic ones.[11, 16, 24-29] However, the scaffolds from aqueous solutions exhibit poorer mechanical properties than those from organic solutions. In addition, people have adopted post-treatment to reinforce the scaffolds, such as immersing in organic solvents, [24, 30, 31] extension,[11, 18, 32] annealing in water vapor[20, 33, 34] or adding some reinforcing agents.[16, 18] However, the post-treated RSF scaffolds in wet state still do not have perfect toughness to be sutured with living tissues such as urethra or bladder.[11] Since bladder acellular matrix graft (BAMG) possesses good physicochemical properties, mechanical reliability and biocompatibility, it has been already used in urethral reconstruction,[35-39] penile reconstruction,[40] myocardial repair,[41] esophageal repair[42] and fascial tissue reconstruction.[43] In this study, we electrospun RSF aqueous solutions on a substrate of BAMG to fabricate composite scaffolds with enhanced mechanical properties. Different post-treatment methods were also applied to induce the conformation transition of RSF.

The vascularization of damaged tissues plays an essential role in the success of tissue regenerating because of vessels providing the

construct not only with nutriments in blood, but also with endothelial progenitor cells.[44, 45] Vascular endothelial growth factor (VEGF) is essential for tissue vasculogenesis and angiogenesis. It also regulates the endothelial cells proliferation, migration and survival to promote the formation of new blood vessels. Because of its short half-life time and rapid clearance, VEGF should be specially delivered and released under control in TE scaffolds to avoid the initial burst release in application. [46, 47]

In this paper, VEGF was encapsulated into RSF fiber by blend and coaxial electrospinning to promote tissue vasculogenesis and angiogenesis, which is important for tissue reconstruction in urethral substitution, myocardial and esophageal repair *etc*. Therefore, porcine iliac endothelial cells (PIECs) were chosen to characterize the bioactivity of released VEGF. For the blend electrospun fiber, VEGF was well dispersed in RSF. For the coaxially electrospun fiber, it had a core-sheath structure with VEGF-bovine serum albumin (BSA) core and RSF sheath. Due to the water-soluble property of as spun RSF scaffolds and controlled release of VEGF, we adopted different strategies to post-treat the composite scaffolds. The morphology, mechanical properties and drug release behaviours of the composite scaffolds with different structures and post-treatments history were investigated. The biocompatibility of the composite scaffolds with PIECs *in vitro* was also demonstrated.

2. Experimental

2.1. Materials

Cocoons of *B. mori* were purchased from Tongxiang, China. Cellulose semipermeable membranes with a molecular weight cutoff 14,000 ± 2000 D were purchased from Yuanju Co., Ltd (Shanghai, China). BAMG was obtained from sacrificed pigs as previously reported,[38] and the detailed preparation of BAMG can be found in Supporting Information.§ BSA was purchased from Sigma-Aldrich Trading Co. Ltd (Shanghai, China). VEGF, trypsin, Dulbecco Modified Eagle's Medium (DMEM) and penicillin-streptomycin were obtained from Gibco Life Technologies Co., USA. Human VEGF ELISA kit was purchased from Raybiotech, Inc. 3-(4, 5-dimethylthiazol-2-yl)-2, 5-diphenyl tetrazolium bromide (MTT) was purchased from Sigma-Aldrich, USA. PIECs (Porcine iliac artery endothelial cell line used in this experiment) were obtained from institute of biochemistry and cell biology (Chinese Academy of Sciences, China). All other chemicals of analytical grade were purchased from Sinopharm Chemical Reagent Co. Ltd. (Shanghai, China).

2.2. Preparation of RSF/VEGF Electrospinning Dopes

Cocoons of *B. mori* were degummed twice with 0.5 wt% Na_2CO_3 aqueous solution at 100 °C for 30 min rinsed with deionized water to remove sericin and dried at room temperature. The dried degummed silk was dissolved in 9.0 M LiBr aqueous solution at 40 °C for 2 h, centrifuged at 3500 rpm for 15 min at 10 °C to remove impurities and diluted with deionized water. Then the RSF aqueous solution was dialyzed against deionized water for 3 days with a cellulose semipermeable membrane to remove the salt and concentrated in forced airflow at 5 °C. Afterwards, VEGF solution (20 μg/mL) was obtained with 2 μg VEGF dissolved in 100 μL 0.1 wt% BSA aqueous solution, and all the samples were stored at -20 °C. For blend electrospinning, 100 μL VEGF solution was added to 16 mL 20 wt% RSF aqueous solution and concentrated to 33 wt% as electrospinning dope. As to coaxial electrospinning, the core electrospinning dope was VEGF-BSA aqueous solution (5 μg/mL) and that of the sheath was RSF aqueous solution (39 wt%). Because it was difficult for coaxial electrospinning to form the core-sheath structure due to water as both the core and sheath electrospinning dopes solvent with low concentration of RSF solution.

2.3. Fabrication of Composite Scaffolds

Before the electrospinning process illustrated in Fig.1, the dried BAMG was stretched smoothly on aluminum foil and wetted with saline to improve its conductivity. Since BAMG is asymmetric, the

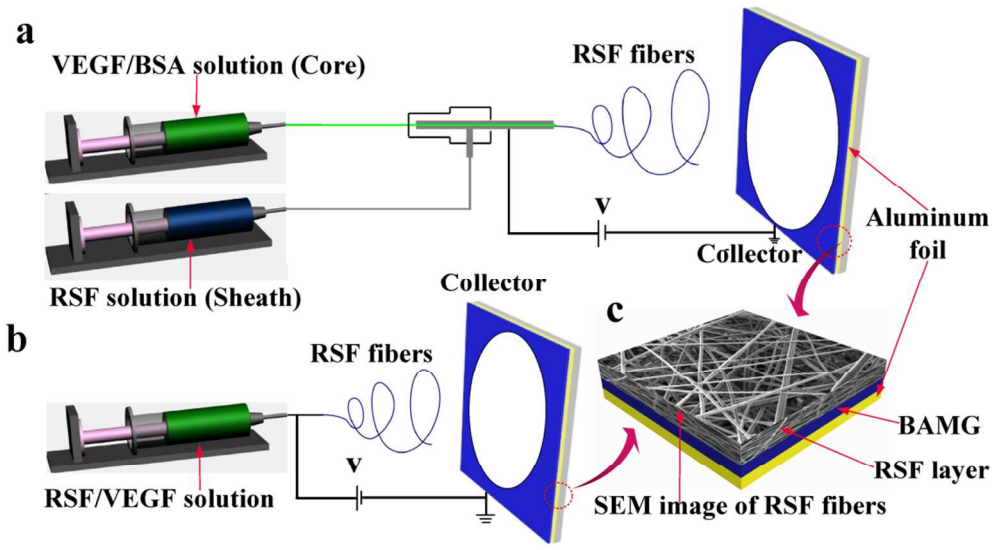

Figure 1. Schematic drawing of (a) coaxial and (b) blend electrospinning of (c) RSF/BAMG composite scaffolds from aqueous solutions

serosal surface of BAMG with dense structure contacted the aluminum foil, while the muscular surface with nanofibers faced air to collect RSF fibers. During the blend electrospinning, VEGF-RSF aqueous solution was spun at a flow rate of 1.2 mL/h using a needle with an inner diameter of 0.6 mm. As to coaxial electrospinning, the core VEGF-BSA aqueous solution and the sheath RSF aqueous solution were spun from inner and outer needles at flow rates of 0.3 and 1.2 mL/h, respectively. The diameters of the inner and outer needles were 0.45 and 2 mm, respectively. The experiments were operated at a voltage of 20 kV and a distance from spinneret to collector of 10 cm for 6 h. Finally, after 15 days drying in air, the scaffolds were peeled off from the collector.

In the further post-treatment process, the as-spun scaffolds were immersed in 90 % (v/v) ethanol for 30 min or annealed in water vapor at 37 °C and 90 % relative humidity for 36 h to induce the conformation transition of RSF.[20, 48] The two methods are environmentally friendly and effective to keep VEGF active. The samples were then dried in air and stored at -20 °C for further study.

2.4. Scanning Electron Microscopy (SEM)

The morphology of the scaffolds was studied by SEM (JEOL JSM-5600LV, Japan). The scaffolds were sputter-coated with platinum and examined at a voltage of 10 kV. The average diameters of the fibers were measured by Image Tool software and more than 100 counts were randomly used for each sample.

2.5. Transmission Electron Microscopy (TEM)

The core-sheath structure of fibers was examined using transmission electron microscope (JEOL JEM-2100, Japan) at a voltage of 200 kV. The samples for TEM were collected by copper grids during the electrospinning process.

2.6. Mechanical Properties

Tensile properties and suture retention strength of the scaffolds (35 mm × 5 mm) were measured in dry and wet states using an Instron 5969 material testing machine at 25 ± 5 °C and 50 ± 5 % of relative humidity. Samples (n=15) were tested at an extension rate of 3 mm/min at a gauge length of 20 mm. In the case of the suture retention strength, the sample was held in the lower grip and threaded with a suture (5–0 Polyglactin, Ethicon, USA) 2mm from its edge. The two ends of the suture were attached to the upper grip. The suture retention was defined as the peak force obtained during this procedure.[49] The thickness of each sample was measured 10 times by a CH-1-S thickness gauge (Shanghai Liuling Instruments Co., Shanghai, China) with a resolution of 1 μm. All samples used in this study are listed in Table 1.

Since silk scaffolds could be fully saturated by immersing in water for more than 10 min,[50] all the samples tested in wet state were soaked beforehand in simulated body fluid (SBF) for 30 min to achieve equilibrium.

2.7. *In Vitro* Release Investigation

The release behaviors of VEGF from different scaffolds (Table 1) were investigated by Human VEGF ELISA Kit. VEGF-loaded scaffolds were weighted 100 mg and immersed into 1mL PBS (n=3). All the specimens were incubated at 37 °C under a dynamic situation (100 rpm). At predetermined intervals (1 d, 2 d, 4 d, 7 d, 10 d, 13 d and 16 d), 400 μL sample was removed for the test, and 400 μL fresh PBS was added. All the samples were collected and stored at -80 °C. VEGF concentrations were then estimated according to a standard curve obtained from an ELISA Kit. Cumulative VEGF release profiles were calculated afterwards.

Table 1. Different samples prepared in this study

Sample code		Post-treatments		VEGF Loaded
		EI	Wva	
BAMG		/	/	/
Bare RSF Scaffolds (without BAMG)	Ble-EI	√	/	/
	Ble-Wva	/	√	/
	Coa-EI	√	/	/
	Coa-Wva	/	√	/
	Ble-EI-VEGF	√	/	√
	Ble-Wva-VEGF	/	√	√
	Coa-EI-VEGF	√	/	√
	Coa-Wva-VEGF	/	√	√
Composite Scaffolds (with BAMG)	Ble-Com-EI	√	/	/
	Ble-Com-Wva	/	√	/
	Coa-Com-EI	√	/	/
	Coa-Com-Wva	/	√	/
Negative Groups	Coverslips	/	/	/
	TCPs	/	/	/

Ble: RSF aqueous solution (33 wt%) for blend electrospinning
Coa: RSF aqueous solution (39 wt%) for coaxial electrospinning
EI: Immersion in 90% (v/v) ethanol for 30 min
Wva: Water vapor annealing at 37 °C and 90% relative humidity for 36 h
√: Applied
/: Not applied

2.8. *In Vitro* Cell Culture and Seeding

Bare RSF scaffolds (Table 1) were punched into circular shape (15 mm in diameter) in 24-well plates and sterilized in 75 vol.% ethanol vapor for 5 h before cell culture experiment. PIECs were seeded at a density of 5×10^3 cells/well, and incubated at 37 °C/5% CO^2. For the cell proliferation study, the proliferation of PIECs on the substrates was quantified on day 1, 3, 5 and 7 by MTT assay. Moreover, TCP_S (tissue cultured polystyrenes) and coverslips were used as negative control groups.

The spreading morphology of PIECs cultured on the scaffolds was also examined by SEM (JEOL JSM-5600LV, Japan). Each group was seeded with PIECs at a density of 8×10^3 cells/well and incubated for 3 days. Afterwards, the samples were rinsed twice with PBS, fixed with 2.5 % glutaraldehyde for 2 h at 4 °C, dehydrated in a graded series of ethanol (30, 50, 70, 80, 90, 95, and 100%). Finally, the dry samples were sputtered with gold and examined.

Moreover, cytoskeletal structure of PIECs cultured on the scaffolds for 3 days was observed using a SP-5 II (LEIKA Co., Germany) laser scanning confocal microscope (LSCM). PIECs were fixed for 2 h with 4% paraformaldehyde at 4 °C, washed by PBS 3 times, and incubated in 0.1% (v/v) Triton-X 100 (Sigma Aldrich) and 1% (v/v) BSA for 5 and 30 min, respectively. Thereafter, samples were stained with Rhodamine labeled phalloidin (1:200) for 20 min. Subsequently, samples were thoroughly washed with PBS and examined. In order to obtain the 3D distribution and spreading morphology of the cells, a stack of images were acquired in the *z* dimension of successive slices and dealt with Imaris 6.2 software (Bitplane Co., Switzerland).

2.9. Statistics and Data Analysis

Typically, the experimental data were represented as mean ± standard deviation. Assays were performed in triplicate. Comparisons between groups were performed by one-way ANOVA tests.[51] In all evaluations, a p-value < 0.05 was considered statistically significant differences between groups.

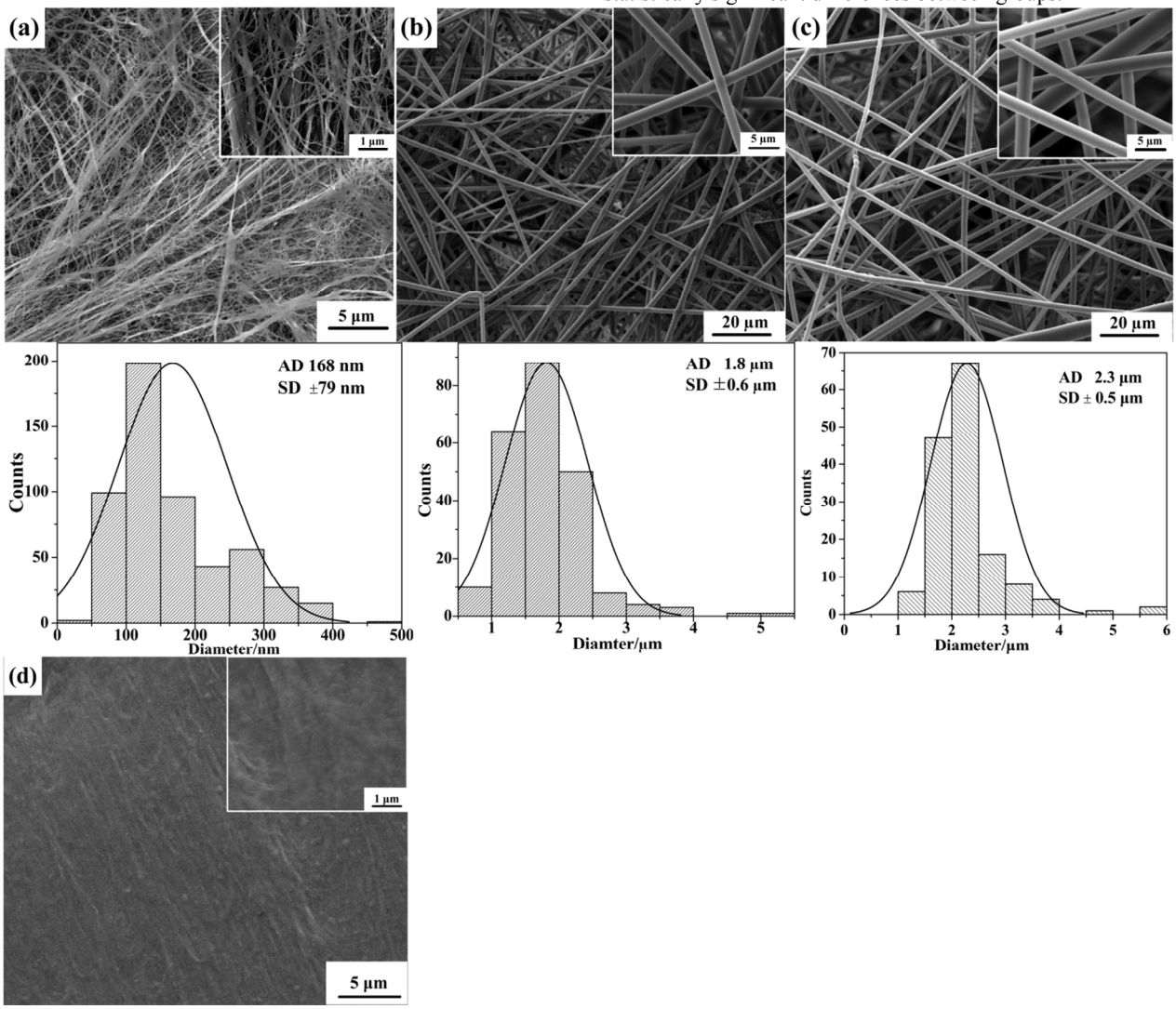

Figure 2. SEM images of (a) the muscular surface of BAMG, (b) blend electrospun composite scaffolds, (c) coaxially electrospun composite scaffolds and corresponding diameter distribution of fibers, and (d) the serosal surface of BAMG

3. Results and discussion

3.1. Morphology of Composite Scaffolds

Fig. 2 shows the SEM images of BAMG and the blend and coaxially electrospun scaffolds. The average diameters of the nanofibers on the muscular surface of BAMG (Fig. 2a), blend (Fig. 2b) and coaxially (Fig. 2c) electrospun fibers were 168 ± 79 nm, 1.8 ± 0.6 μm and 2.3 ± 0.5 μm, respectively. During the electrospinning process, the BSA-VEGF aqueous solution in the core could have effects on the size of the coaxially electrospun fibers, leading to difference in the fiber diameters and distribution between blend and coaxially electrospun fibers. We can also see that the serosal surface of BAMG (Fig. 2d) is smoother than the muscular surface (Fig. 2a). So we used muscular surface to collect RSF fibers, which could adhere BAMG firmly.

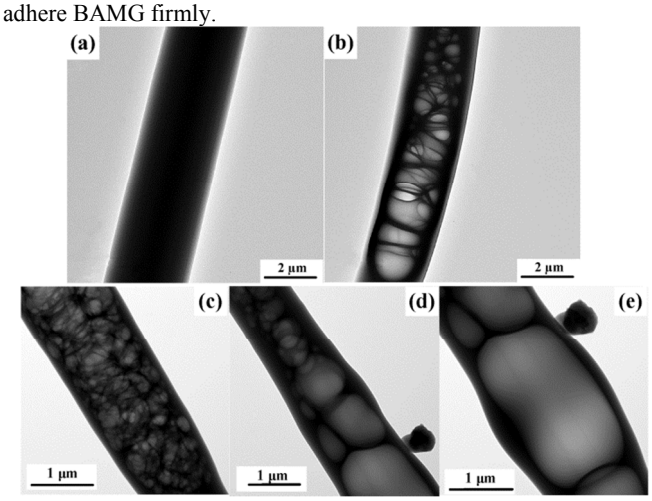

Figure 3. TEM images of (a) blend electrospun fiber of RSF and VEGF, (b-e) coaxially electrospun fiber of RSF and BSA-VEGF. The flow rates of the core and sheath spinning dopes of (b) are 0.3 and 1.2 mL/h, respectively. The flow rates of the core and sheath spinning dopes of (c-e) are 0.6 and 1.8 mL/h, respectively. TEM images (c-e) were taken at different positions of the coaxial fiber.

As shown in Fig. 3, TEM images show that the blend electrospun fiber (Fig. 3a) was solid, while there was bubble structure between core and sheath layers for the coaxially electrospun fiber with different flow rates of core and sheath spinning dopes (Fig. 3b-e). There might be two reasons for the bubble structure. Since the coaxial electrospinning process is very fast and the water content in the core spinning dope is high, BSA-VEGF solution in the core might not volatilize thoroughly. The residual solution might dissolve some RSF sheath and volatilize to the bubbles at a high temperature resulted from the electron beam on the fiber. The bubble structure (Fig. 3c-e) also occurred more apparent due to more residual water in the core in the case of the core/sheath flow rates of 0.6/1.8 mL/h. Since the extending irradiation time of the electron beam on the fiber may result in the raise of the temperature, the water volatilization in the core may make the bubbles (Fig. 3c-e) expand at the different positions of the coaxial fiber. The bubble structure might be also attributed to the degrading effects of the high energy electron beam on the fiber. However, as we can see from Fig. 3a, the blend electrospun fiber did not have the bubble structure at the same voltage as used in the TEM observation for the coaxial fiber. So we thought that the water volatilization in the core was more reasonable for the bubble structure formation than the degrading effects of the electron beam.

3.2. Mechanical Properties

3.2.1. Tensile Properties

The thickness of BAMG, bare RSF scaffolds and RSF/BAMG composite scaffolds were 30 ± 10 μm, 120 ± 20 μm and 150 ± 30 μm, respectively. Fig. 4 shows the mechanical properties of BAMG, RSF scaffolds and BAMG/RSF composite scaffolds listed in Table 1 in dry and wet states. This indicates that BAMG (Fig. 4A) in dry state possessed high breaking strength of 41.1 ± 10.8 MPa and elongation at break of 21.1 ± 2.2%, which were much higher than those of bare RSF scaffolds (Fig. 4B). Comparing Fig. 4B with 4C, we can see that both the breaking strength and elongation at break of the composite scaffolds were much higher than the counterpart without BAMG, which proved that the mechanical properties of the composite scaffolds were significantly improved by compositing a BAMG layer. From the detailed mechanical properties shown in Table S1§ (Supporting Information), it is known that the breaking energy of the composite scaffolds (Ble-Com-Wva) reached 970.8 and 681.7 $J \cdot kg^{-1}$ in dry and wet states with the combination of BAMG, respectively. Compared with the bare scaffolds (61.2 $J \cdot kg^{-1}$ of Ble-Wva in dry state), the drastically toughened Ble-Com-Wva exhibited at least 10-fold increase in breaking energy.

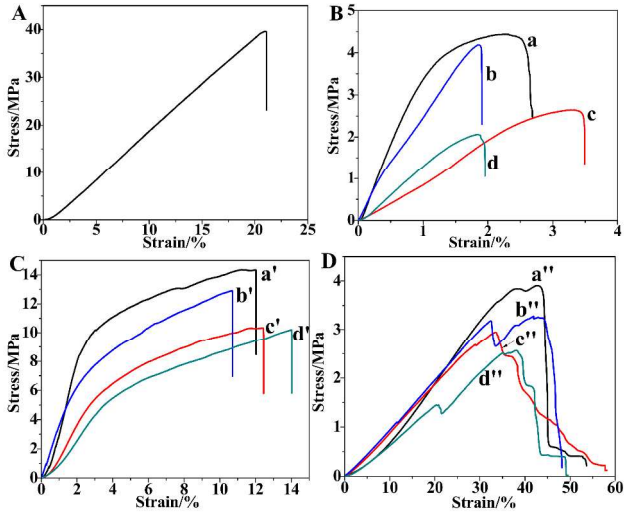

Figure 4. Stress–strain curves of (A) BAMG and (B) bare scaffolds in dry state: (a) Ble-Wav, (b) Coa-Wav, (c) Ble-EI and (d) Coa-EI, respectively. Stress–strain curves of the blend and coaxially electrospun composite scaffolds with different post-treatments in (C) dry and (D) wet states: (a', a") Ble-Com-Wav, (b', b") Coa-Com-Wav, (c', c") Ble-Com-EI and (d', d") Coa-Com-EI, respectively.

It can be found from Fig. 4B that the breaking strength of Ble-Wva (curve a) and Ble-EI (curve c) was higher than those of Coa-Wva (curve b) and Coa-EI (curve d) in dry state, respectively. This indicates that the blend electrospun scaffolds were stronger than the coaxial samples. The principle could also be found from the composite scaffolds shown in Fig. 4C, which was attributed to the different structures of the blend and coaxially electrospun fibers shown in Fig. 3. The blend electrospun fibers were solid (Fig. 3a),

while the coaxial fibers were made up of hollow core and solid sheath (Fig. 3b). It was also known from Fig. 4B that the breaking strengths of the blend and coaxially electrospun RSF scaffolds annealed in water vapor of (Ble-Wva, curve a; Coa-Wva, curve b) were higher than those immersed in ethanol (Ble-EI, curve c; Coa-EI, curve d), respectively. Fig. 4C and Fig. 4D show the similar results for the composite scaffolds in dry and wet states. Analysis of Fourier Transform infrared (FTIR) spectra of different RSF scaffolds (Fig. S1§) show that both water vapor annealing and immersion in ethanol could promote the structure of RSF transforming from α-helix/random coil (1536 cm^{-1}, 1545 cm^{-1}) to β-sheet (1515 cm^{-1},1623 cm^{-1}), which related to the crystallization of RSF. The RSF scaffolds annealed in water vapor possess higher content of β-sheet than the scaffolds immersed in ethanol (Table S2§). Since the molecular size of water is much smaller than ethanol, it is much easier for the water to enter the matrix of RSF molecules, break the intra-molecular H-bonds (α-helix) and form the inter-molecular H-bonds (β-sheet) of RSF. The higher post-treatment temperature (37 ^{o}C) and longer post-treatment time (36 h) in the water vapor annealing process also accelerate the conformation transition of RSF from α-helix/random coil to β-sheet.[34,52] Wide angle X-ray diffraction (WAXD) results (Fig. S2§) shows that the two post-treatments could improve the crystallinity of the RSF scaffolds. Compared with immersion in ethanol (c and d), water vapor annealing significantly improved the crystallinity of the RSF scaffolds (e and f), which were important to the mechanical properties. The crystallinity of the RSF scaffolds agreed with the analysis of β-sheet results. Thus, it was concluded that water vapor annealing was a better post-treatment than immersion in ethanol, because water vapor annealing was a mild strategy to enhance the mechanical properties.[20, 34]

From Fig. 4C and 4D, we can see that the breaking strength of composite scaffolds in wet state ranges from 2.6 to 3.9 MPa, while the dry counterparts exhibit a breaking strength ranging from 10.2 to 14.4 MPa. In the meantime, the elongation at break in wet state was much higher than that in dry state, which ranged from 48.2 % to 58.2 %. Regardless of the dry or wet state during testing, the strength of the blend electrospun scaffolds was higher than that of the coaxially electrospun scaffolds post-treated at the same condition. Because the structures between the blend and coaxially electrospun fibers were different, the bubble structure shown in Fig. 3 b may weaken the coaxially electrospun fibers.

Park *et al*[20] electrospun non-woven matrices from RSF/1,1,1,3,3,3-hexafluoro-2-propanol (HFIP) solution. The methanol-immersed and water vapor annealed RSF scaffolds showed breaking strength of 2.6 and 4.6 MPa, and elongation at break of 8.5% and 4.4 %, respectively. Pan[16] adopted deionized water as solvent and added multiwalled carbon nanotubes (MWNTs) to fabricate the reinforced elctrospun SF mats with a breaking strength and a elongation at break of 3.5 MPa and 2.5 %, respectively. Sheida[53] made a hybrid scaffolds of SF/poly(lactide-co-glycolic acid) (PLGA) with a breaking strength and an elongation at break of 1.85 MPa and 15.2 %, respectively. Fan[11] electrospun RSF mats from RSF aqueous solution with a breaking strength of 8.6 MPa and an elongation of 4.6 % after stretching and immersion in ethanol. Jiang[54] fabricated RSF scaffolds with aligned electrospun fibers in multiple layers. The breaking strength and elongation at break of the scaffolds were 7.6 MPa and 3.2 % after immersion in ethanol. However, all the scaffolds mentioned above are weaker than our RSF/BAMG composite scaffolds.

Liu[55] used RSF/$CaCl_2$/formic acid solution to electrospin nanofibers scaffolds. After ethanol treatment, the breaking strength and elongation at break of the scaffolds were 11.15 MPa and 7.66 % in dry state, and 3.32 MPa and 174.0 % in wet state, respectively. Although their mechanical properties were close to our RSF/BAMG composite scaffolds, the residual organic solvent in the scaffolds might be unfriendly to the cells in tissue. Gandhi[18] electrospun scaffolds with RSF/formic acid/single walled carbon nanotubes (CNT) solution. After methanol and stretching post-treatment, it shows that the breaking strength and elongation at break were 44.5 MPa and 1.2 %, respectively. The brittle characteristics make it hard to suture with tissue despite of the high breaking strength. Moreover, there was still residual organic solvent in the scaffolds.

3.2.2. Suture Retention Strength

In some occasions, scaffolds need to be sutured with some damaged tissue, such as urethral or bladder. Thus the suture retention strength was a crucial factor to the success of the composite scaffolds during implantation procedure. Table 2 shows the suture retention strength of BAMG and post-treated scaffolds in dry and wet states, respectively.

Table 2. Suture retention strength of BAMG and post-treated scaffolds in dry and wet states

Sample code	Suture retention (N)	
	dry state	wet state
BAMG	1.4 ± 0.1	1.1 ± 0.1
Ble-EI	1.2 ± 0.2^{b1}	/
Ble-Wva	1.3 ± 0.3^{b2}	/
Coa-EI	1.0 ± 0.2^{c1}	/
Coa-Wva	1.1 ± 0.2^{c2}	/
Ble-Com-EI	$4.4 \pm 1.4^{b1**}$	$2.1 \pm 0.5^{b1**}$
Ble-Com-Wva	$4.5 \pm 1.0^{b2**}$	$2.3 \pm 0.4^{b2**}$
Coa-Com-EI	$4.1 \pm 0.9^{c1**}$	$2.0 \pm 0.3^{c1**}$
Coa-Com-Wva	$4.3 \pm 0.9^{c2**}$	$2.0 \pm 0.3^{c2**}$

b1: the Suture retention strength of blend electrospun scaffolds immersed in ethanol
b2: the Suture retention strength of blend electrospun scaffolds annealed in water vapor
c1: the Suture retention strength of coaxially electrospun scaffolds immersed in ethanol
c2: the Suture retention strength of coaxially electrospun scaffolds annealed in water vapor
**: Comparisons between the same kind of post-treated group, p-value < 0.01.

In dry state, the BAMG showed suture retention strength of 1.4 ± 0.1 N, while the pure RSF scaffolds exhibited a little bit lower suture retention strength ranging from 1.0 to 1.2 N according to different post-treatment methods. Although the tensile strength of the BAMG was good, its suture retention strength was close to those of RSF scaffolds due to the thickness of only 30 ± 10 μm, which was 3 times thinner than RSF scaffolds. Compared with RSF scaffolds, the thickness of the composite scaffolds was increased by about 30 μm while their suture retention strength was increased a lot from 4.1 to 4.5 N. For both the RSF and composite scaffolds, the suture retention strength of blend electrospun scaffolds was higher than that of coaxially electrospun scaffolds because of different structures of fibers (Fig. 3). For both blend and coaxially electrospun scaffolds, the suture retention strength of water vapor annealed scaffolds was higher than that of ethanol-immersed scaffolds, which meant water vapor annealing was a better post-treated method. This is consistent with the results of tensile strength of the scaffolds.

In wet state, the suture retention strength of the BAMG was 1.1 ± 0.1 N, which was a little bit lower than that in dry state. However, the suture retention strength of the composite scaffolds was decreased a lot compared in dry state, which was ranging from 2.0 to 2.3 N. Moreover, the suture retention strength of the blend electrospun scaffolds was a little higher than that of the coaxially electrospun scaffolds post-treated at the same condition. This may also attribute to the bubble structures shown in Fig. 3 b. However, the suture retention strength is still higher than 2.0 N in wet state,[49] which was generally accepted to require for suturing with tissue in implantation

3.3. Release Behaviors of VEGF

Fig. 5B shows the cumulative release profiles of VEGF from different scaffolds with different post-treatments. Fig. 5A and 5C are VEGF release schematics of the blend and coaxially electrospun fibers, respectively. As we can see from the tendency of the curves (Fig. 5B), the release profiles of VEGF evidently increased with time and have continued for more than 16 days. This indicates a successfully sustained release of VEGF as Huang reported.[56] Furthermore, there was no obvious burst release that all the loaded VEGF released in first day during the sustained release. It meant all the samples were suitable for drug delivery and controlled release.

Comparing the two types of post-treatments, we found that there was an obvious difference between immersion in the ethanol and water vapor annealing, especially for the blend electrospun composite scaffolds. As shown in Fig. 5B, the profiles of released VEGF of the samples annealed in water vapor (curves a and b) were higher than those immersed in ethanol (curves c and d). It was proved that water vapor annealing was a mild process for VEGF release, while ethanol might be harmful to VEGF or inactivate some VEGF. Since ethanol induces denaturation of protein, such as the enzyme and human serum albumin,[57, 58] VEGF, as a kind of protein, might also be influenced by the ethanol. However, the water vapor at 37°C mimics human body environment and water is a green solvent for protein drugs. Thus, water vapor annealing was a milder method to keep VEGF active than immersion in ethanol. In addition, VEGF release profile of the blend electrospun scaffolds (Fig. 5B (a)) was much higher than the coaxial counterpart (Fig. 5B (b)). This was resulted from the different loaded amount of VEGF and different structures of the blend and coaxially electrospun scaffolds. The amount of VEGF loaded in the blend electrospun scaffolds was about twice as that in the coaxially electrospun scaffolds. For the blend electrospun fiber (Fig. 5A), we can see that VEGF was evenly dispersed in the fiber. While for the coaxially electrospun scaffolds (Fig. 5C), VEGF was dispersed only in the core of the fibers. Thus VEGF needed more time to release to the outer RSF sheath of the fibers. Due to the above two reasons, VEGF released more continuously from the coaxially electrospun fibers than the blend samples. Moreover, VEGF release difference between the coaxially electrospun samples with two kinds of post-treatments was smaller than the blend ones due to the existence of RSF sheath, which contributed to the sustained release for a long time.

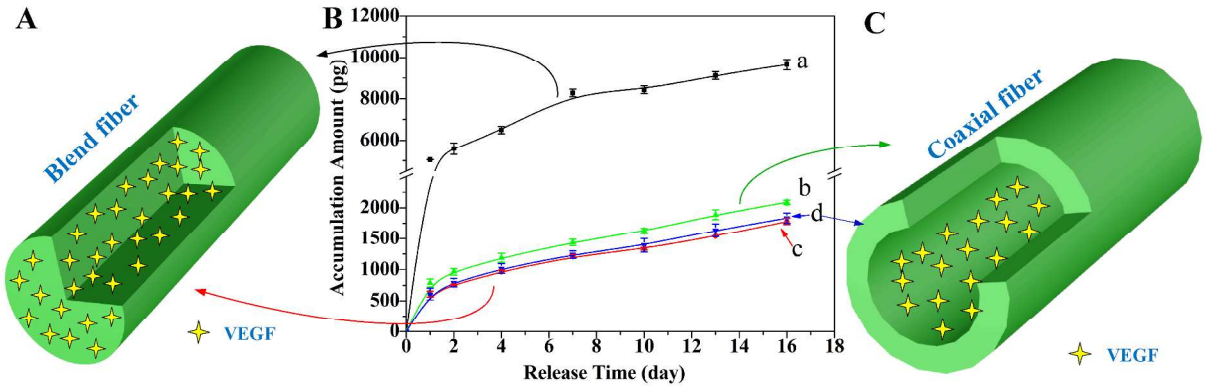

Figure 5. VEGF release schematics and profiles (B) of (A) blend and (C) coaxially electrospun fibers: (a) Ble-Wva-VEGF, (b) Coa-Wva-VEGF, (c) Ble-EI-VEGF and (d) Coa-EI-VEGF, respectively.

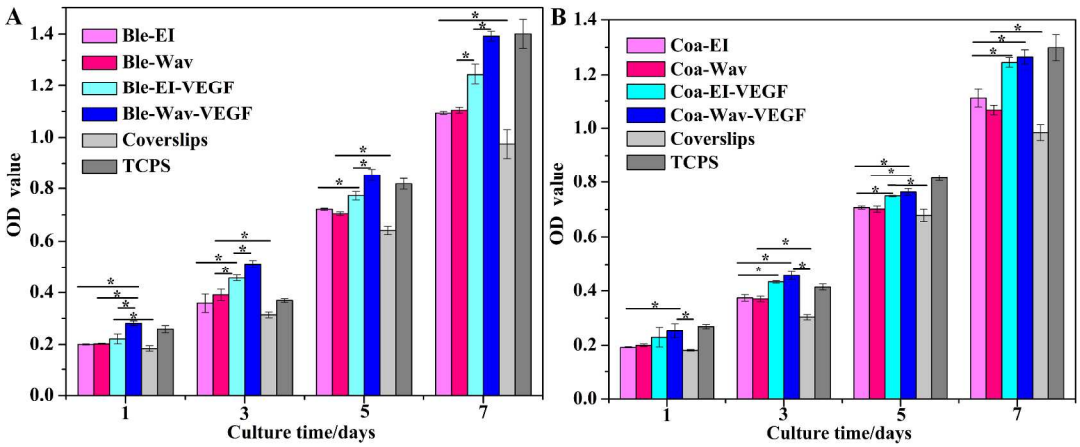

Figure 6. MTT OD value of PIECs proliferation cultured on the blend (A) and coaxially (B) electrospun scaffolds for 7 days (*p< 0.05).

3.4. In Vitro Bioactivity Study

The bioactivity of released VEGF was analyzed by observing the growth of PIECs cultured on the scaffolds loaded with VEGF. Fig. 6 is cell proliferation of PIECs cultured on the (A) blend and (B) coaxially electrospun scaffolds, respectively. We can see that all the evaluated conditions revealed an obviously increased proliferation of the electrospun scaffolds, which proved the scaffolds exhibited good cytobiocompatibility. Moreover, both the blend and coaxial mats encapsulated VEGF (Ble-EI-VEGF, Ble-Wva-VEGF, Coa-EI-VEGF, Coa-Wva-VEGF) show faster cell proliferation than those without VEGF (Ble-EI, Ble-Wva, Coa-EI, Coa-Wva). Within 7 days, it was significant difference between groups with a value *p < 0.05. On day 7, it shows an obvious effect of VEGF on the cell proliferation between the scaffolds with or without it. This indicates that the released VEGF kept bioactive for 7 days and the introduction of released VEGF could promote fast proliferation of PIECs on the scaffolds.[8] From the OD values, we also can see that there was significant difference between the blend electrospun groups annealed water vapor and immersed in ethanol with VEGF within 7 days, which showed better cell proliferation of the samples annealed water vapor (Ble-EI-VEGF, Ble-Wva-VEGF). It also indicates that water vapor annealing was a better to keep VEGF active than immersion in ethanol. The difference between the blend electrospun groups was about 10 % at most on day 7. For the coaxial samples, there was no significant difference between the two kinds of scaffolds with VEGF (Coa-EI-VEGF, Coa-Wva-VEGF). This is consistent with the results of VEGF release curves in Fig. 5B. Comparing with the samples without VEGF, we can find that there was no significant difference in cell proliferation for the two post-treated strategies.

Fig. 7 shows the SEM images of PIECs cultured on the blend and coaxially electrospun scaffolds post-treated using different methods, respectively. As demonstrated in these figures, we can find that PIECs could adhere and stretch well on both blend and coaxial samples. In addition, for VEGF-loaded scaffolds, there were obviously more cell confluence observed in images c and d (Fig. 7 Ble and Coa SEM) than those without VEGF in images a and b (Fig. 7 Ble and Coa SEM). This is consistent with the trend of aforementioned MTT assay results presented in Fig. 6. Comparing images c with d (Fig. 7 Ble and Coa SEM), we can see that there were more cells adhered on the water vapor annealed scaffolds than those immersed in ethanol. This agrees with the result of VEGF release in Fig. 5B.

As shown in Fig. S3§ A and B in Supplementary Data, the cell phenotype was validated in 2D LSCM images of the blend and coaxially electrospun scaffolds, respectively. The Rhodamine-labeled cell (Red) presented similar results to cell spreading (Fig. 7 Ble and Coa SEM). The results suggest that cells on the VEGF-releasing samples in images c and d exhibited more positive and active for cell attachment than those without VEGF in images a and b (Fig. S3§ A and B). It could be known that the released VEGF kept bioactive to promote PIECs spreading and proliferating on the scaffolds.

In addition, cell cytoskeletal structure in the scaffolds was observed by 3D LSCM images (Fig. 7 Ble and Coa LSCM 3D). It was a drawback that dense structure and fine pores limited cells ingrowth into the scaffolds which was difficult to establish an even 3-D distribution of cells.[46, 59] From LSCM 3D images in this experiment, we can see that PIECs could not only grow on the surface of the scaffolds, but also infiltrate into them. The good permeability was an important property of the scaffolds. The cell adhesion and proliferation results observed from Fig. 7 LSCM 3D images agree with those of MTT assay in Fig. 6 A and B. This study proved that the scaffolds were suitable for cell adhesion, proliferation and infiltration, and meant that the scaffolds could satisfy the needs as TE scaffolds for applications. [60]

4. Conclusions

The current study described the preparation and characterization of VEGF-loaded RSF/BAMG electrospun composite scaffolds by means of blend and coaxial electrospinning. Tensile and suture tests analysis showed that the reinforced composite scaffolds, especially those post-treated with water vapor annealing, exhibited significantly better mechanical properties than those without BAMG, which

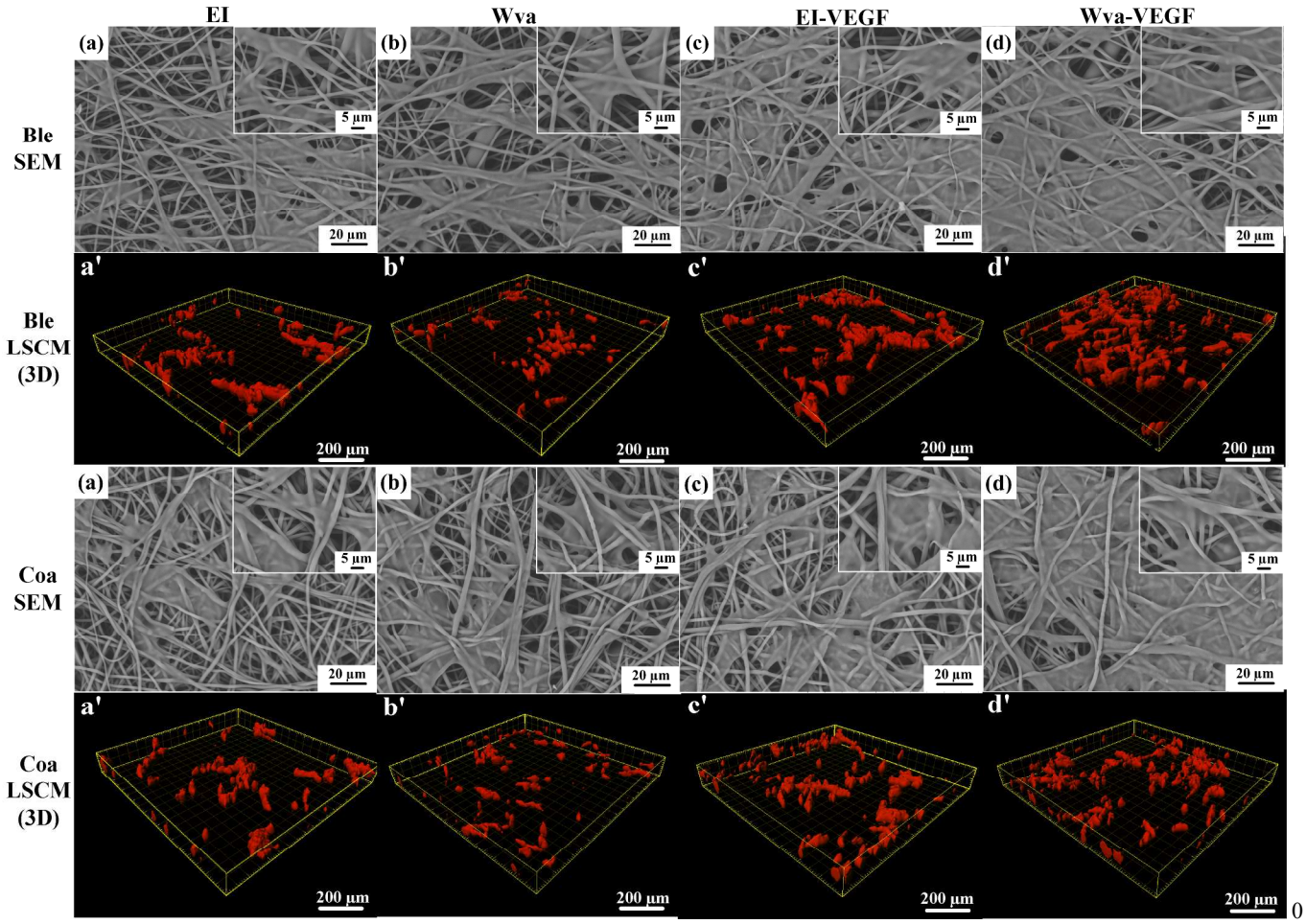

Figure 7. PIECs spreading and cytoskeletal structure on the blend and coaxially electrospun scaffolds. SEM and LSCM 3D (Rhodamine labeled) images of PIECs cultured on the blend (Ble) and coaxially (Coa) electrospun scaffolds for 3 days. All scaffolds were post-treated using different methods of EI and Wva, respectively. Furthermore, the cell spreading was observed on different scaffolds cultured for 3 days by SEM.

satisfied the requirements of TE scaffolds for implantation. VEGF was successfully loaded into the electrospun scaffolds with sustained release. Compared with immersion in ethanol, water vapor annealing is more appropriate to enhance the mechanical properties of the composite scaffolds and maintain the bioactivity of VEGF. The released VEGF preserved its bioactivity to support PIECs growth up to at least 7 days. PIECs could adhere, spread and proliferate well on the scaffolds, and even infiltrate into the scaffolds. These RSF/BAMG bioactive blend and coaxially electrospun composite scaffolds were successful to deliver and release VEGF in a sustained manner, and could be considered as attractive candidates for TE applications. In addition, this study has proved that we can use physical ways to fabricate composite scaffolds with good mechanical properties and biocompatibility instead of using organic agents, which provides a new method to fabricate TE scaffolds. To further understand the biomechanical properties of the composite scaffolds for intended organ/system, *in vivo* experiments are still needed be performed in some tissues and organs, such as vascular, skin, orthopaedic or genitourinary *etc*.

Acknowledgements

This work is supported by the National Natural Science Foundation of China (21274018, 81170641), the Innovation Program of the Shanghai Municipal Education Commission (12ZZ065), China Postdoctoral Science Foundation (2014M551293), the Programme of Introducing Talents of Discipline to Universities (No.111-2-04), DHU Distinguished Young Professor Program (A201302), the Fundamental Research Funds for the Central Universities and State Key Laboratory for Modification of Chemical Fibers and Polymer Materials, Donghua University (LK1408). We also acknowledge Mrs. Mengxia Chen for her help in *in vitro* experiments.

Notes and references

[a] State Key Laboratory for Modification of Chemical Fibers and Polymer Materials, College of Materials Science and Engineering, Donghua University, Shanghai 201620, P.R. China.
E-mail: zyp@dhu.edu.cn; Fax: +86-21-67792955; Tel: +86-21-67792954
[b] Department of Urology, Shanghai Jiao Tong University Affiliated Sixth People's Hospital, Shanghai 200233, P. R. China.
[c] College of Chemistry, Chemical Engineering and Biotechnology, Donghua University, Shanghai 201620, P.R. China.
§ Electronic Supplementary Information (ESI) available: [The method to prepare BAMG, mechanical properties of BAMG and post-treated scaffolds in dry and wet states, FTIR and WAXD results of the RSF scaffolds with different post-treatments, and LSCM 2D images of Rhodamine labeled PIECs]. See DOI: 10.1039/b000000x/

1. T. Dvir, B. P. Timko, D. S. Kohane and R. Langer, *Nat. Nanotechnol.*, 2011, **6**, 13-22.
2. H. Seyednejad, W. Ji, F. Yang, C. F. van Nostrum, T. Vermonden, J. J. J. P. van den Beucken, W. J. A. Dhert, W. E. Hennink and J. A. Jansen, *Biomacromolecules*, 2012, **13**, 3650-3660.
3. X. H. Zhang, M. R. Reagan and D. L. Kaplan, *Adv. Drug Delivery Rev.*, 2009, **61**, 988-1006.
4. S. G. Kumbar, R. James, S. P. Nukavarapu and C. T. Laurencin, *Biomed. Mater.*, 2008, **3**, 034002.
5. A. Greiner and J. H. Wendorff, *Angew. Chem. Int. Ed.*, 2007, **46**, 5670-5703.
6. M. Y. Li, M. J. Mondrinos, M. R. Gandhi, F. K. Ko, A. S. Weiss and P. I. Lelkes, *Biomaterials*, 2005, **26**, 5999-6008.
7. S. Agarwal, J. H. Wendorff and A. Greiner, *Polymer*, 2008, **49**, 5603-5621.
8. H. Zhang, X. Jia, F. Han, J. Zhao, Y. Zhao, Y. Fan and X. Yuan, *Biomaterials*, 2013, **34**, 2202-2212.
9. C. Vepari and D. L. Kaplan, *Prog. Polym. Sci.*, 2007, **32**, 991-1007.
10. T. Arai, G. Freddi, R. Innocenti and M. Tsukada, *J. Appl. Polym. Sci.*, 2004, **91**, 2383-2390.
11. S. Fan, Y. Zhang, H. Shao and X. Hu, *Int. J. Biol. Macromol.*, 2013, **56**, 83-88.
12. G. H. Altman, F. Diaz, C. Jakuba, T. Calabro, R. L. Horan, J. Chen, H. Lu, J. Richmond and D. L. Kaplan, *Biomaterials*, 2003, **24**, 401-416.
13. R. L. Horan, K. Antle, A. L. Collette, Y. Wang, J. Huang, J. E. Moreau, V. Volloch, D. L. Kaplan and G. H. Altman, *Biomaterials*, 2005, **26**, 3385-3393.
14. J. Zhou, C. Cao and X. Ma, *Int J Biol Macromol*, 2009, **45**, 504-510.
15. J. Chutipakdeevong, U. R. Ruktanonchai and P. Supaphol, *J. Appl. Polym. Sci.*, 2013, **130**, 3634-3644.
16. H. Pan, Y. Zhang, Y. Hang, H. Shao, X. Hu, Y. Xu and C. Feng, *Biomacromolecules*, 2012, **13**, 2859-2867.
17. K.-H. Kim, L. Jeong, H.-N. Park, S.-Y. Shin, W.-H. Park, S.-C. Lee, T.-I. Kim, Y.-J. Park, Y.-J. Seol, Y.-M. Lee, Y. Ku, I.-C. Rhyu, S.-B. Han and C.-P. Chung, *J. Biotechnol.*, 2005, **120**, 327-339.
18. M. Gandhi, H. Yang, L. Shor and F. Ko, *Polymer*, 2009, **50**, 1918-1924.
19. S. Sukigara, M. Gandhi, J. Ayutsede, M. Micklus and F. Ko, *Polymer*, 2003, **44**, 5721-5727.
20. B.-M. Min, L. Jeong, K. Y. Lee and W. H. Park, *Macromol. Biosci.*, 2006, **6**, 285-292.
21. S. Zarkoob, R. Eby, D. H. Reneker, S. D. Hudson, D. Ertley and W. W. Adams, *Polymer*, 2004, **45**, 3973-3977.
22. Y. Kawahara, A. Nakayama, N. Matsumura, T. Yoshioka and M. Tsuji, *J. Appl. Polym. Sci.*, 2008, **107**, 3681-3684.
23. K. Ohgo, C. Zhao, M. Kobayashi and T. Asakura, *Polymer*, 2003, **44**, 841-846.
24. H. Cao, X. Chen, L. Huang and Z. Shao, *Mater. Sci. Eng., C*, 2009, **29**, 2270-2274.
25. J. Zhu, H. Shao and X. Hu, *Int. J. Biol. Macromol.*, 2007, **41**, 469-474.
26. J. Zhu, Y. Zhang, H. Shao and X. Hu, *Polymer*, 2008, **49**, 2880-2885.
27. Y. Hang, Y. Zhang, Y. Jin, H. Shao and X. Hu, *Int. J. Biol. Macromol.*, 2012, **51**, 980-986.
28. H. Wang, H. Shao and X. Hu, *J. Appl. Polym. Sci.*, 2006, **101**, 961-968.
29. H. Wang, Y. Zhang, H. Shao and X. Hu, *J. Mater. Sci.*, 2005, **40**, 5359-5363.
30. M. Wang, H.-J. Jin, D. L. Kaplan and G. C. Rutledge, *Macromolecules*, 2004, **37**, 6856-6864.
31. C. Chen, C. Chuanbao, M. Xilan, T. Yin and Z. Hesun, *Polymer*, 2006, **47**, 6322-6327.
32. J. Yin, E. Chen, D. Porter and Z. Shao, *Biomacromolecules*, 2010, **11**, 2890-2895.
33. X. Hu, K. Shmelev, L. Sun, E.-S. Gil, S.-H. Park, P. Cebe and D. L. Kaplan, *Biomacromolecules*, 2011, **12**, 1686-1696.
34. X. Huang, S. Fan, A. I. M. Altayp, Y. Zhang, H. Shao, X. Hu, M. Xie and Y. Xu, *J. Nanomater.*, 2014, DOI:10.1155/2014/682563.
35. S. Dahms, H. Piechota, R. Dahiya, T. Lue and E. Tanagho, *British J. Urology*, 1998, **82**, 411-419.
36. M. Youssif, H. Shiina, S. Urakami, C. Gleason, L. Nunes, M. Igawa, H. Enokida, E. A. Tanagho and R. Dahiya, *Urology*, 2005, **66**, 201-207.
37. H. Li, Y. Xu, H. Xie, C. Li, L. Song, C. Feng, Q. Zhang, M. Xie, Y. Wang and X. Lv, *Tissue Eng. Pt. A*, 2014.
38. C. Feng, Y.-M. Xu, Q. Fu, W.-D. Zhu, L. Cui and J. Chen, *J. Biomed. Mater. Res. A*, 2010, **94A**, 317-325.
39. C. Li, Y.-M. Xu and H.-B. Li, *Asian J. Androl.,* 2013, **15**, 430-433.
40. K. J. Joo, B. S. Kim, J. H. Han, C. J. Kim, C. H. Kwon and H. J. Park, *Asian J. Androl.*, 2006, **8**, 543-548.
41. S. Badylak, J. Obermiller, L. Geddes, and R. Matheny, *Heart. Surg. Forum*, 2003, **6**, E20-E26.
42. S. Badylak, S. Meurling, M. Chen, A. Spievack, and A. Simmons-Byrd, *J. Pediatr. Surg.*, 2000, **35**, 1097-1103.
43. D. Eberli, A. Atala and J. J. Yoo, *J. Mater. Sci.: Mater. Med.*, 2011, **22**, 741-751.
44. C. D. Gaudio, S. Baiguera, M. Boieri, B. Mazzanti, D. Ribatti, A. Bianco and P. Macchiarini, *Biomaterials*, 2013, **34**, 7754-7765.
45. Z. K. Otrock, J. A. Makarem and A. I. Shamseddine, *Blood Cells, Mol., Dis.*, 2007, **38**, 258-268.
46. F. X. Han, X. L. Jia, D. D. Dai, X. L. Yang, J. Zhao, Y. H. Zhao, Y. B. Fan and X. Y. Yuan, *Biomaterials*, 2013, **34**, 7302-7313.
47. Y.-I. Chung, S.-K. Kim, Y.-K. Lee, S.-J. Park, K.-O. Cho, S. H. Yuk, G. Tae and Y. H. Kim, *J. Controlled Release*, 2010, **143**, 282-289.
48. K.-H. Zhang, Q. Ye and Z.-Y. Yan, *Int. J. Mol. Sci.*, 2012, **13**, 2036-2047.
49. K. Billiar, J. Murray, D. Laude, G. Abraham and N. Bachrach, *J. Biomed. Mater. Res.*, 2001, **56**, 101-108.
50. F. Han, S. Liu, X. Liu, Y. Pei, S. Bai, H. Zhao, Q. Lu, F. Ma, D. Kaplan and H. Zhu, *Acta Biomater.*, 2014, **10**, 921-930.
51. O. Oliviero, M. Ventre and P. Netti, *Acta Biomater.*, 2012, **8**, 3294-3301.

52. J. Nam and Y. H. Park, *J. Appl. Polym. Sci*, 2001, **81**, 3008-3021.
53. S. Shahverdi, M. Hajimiri, M. A. Esfandiari, B. Larijani, F. Atyabi, A. Rajabiani, A. R. Dehpour, A. A. Gharehaghaji and R. Dinarvand, *Int. J. Pharm.*, 2014, **473**, 345-355.
54. N. Jiang, X. Huang, Z. Li, L. Song, H. Wang, Y. Xu, H. Shao and Y. Zhang, *RSC Adv.*, 2014, **4**, 47570-47575.
55. Z. Liu, F. Zhang, J. F. Ming, S. Y. Bie, J. J. Li and B. Q. Zuo, *J. Appl. Polym. Sci.*, 2015, **132**.
56. M. Huang, S. N. Vitharana, L. J. Peek, T. Coop and C. Berkland, *Biomacromolecules*, 2007, **8**, 1607-1614.
57. A. K. G. Elena V. Kudryashova, Alexander V. Vakurov, and A. L. Frederic Heitz, Vadim V. Mozhaev, *Biotechnol. Bioeng.*, 1997, **55**, 267-277.
58. S. Y. Lin, M. J. Li and Y. S. Wei, *Spectrochim. Acta A*, 2004, **60**, 3107-3111.
59. M. J. McClure, P. S. Wolfe, D. G. Simpson, S. A. Sell and G. L. Bowlin, *Biomaterials*, 2012, **33**, 771-779.
60. Y. Wang, H.-J. Kim, G. Vunjak-Novakovic and D. L. Kaplan, *Biomaterials*, 2006, **27**, 6064-6082.

For Table of Contents Use Only

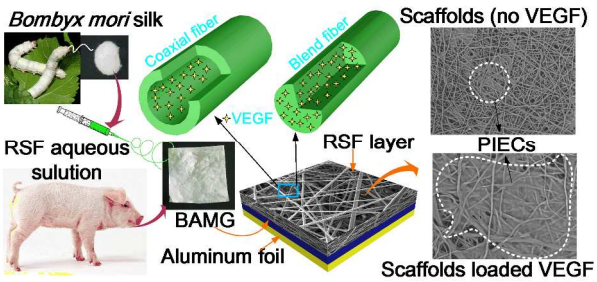

The blend and coaxially electrospun RSF/BAMG composite scaffolds loaded VEGF exhibited good cell compatibility with improved mechanical properties.